Published in final edited form as:
Nat Mater. 2010 December ; 9(12): 1004–1009. doi:10.1038/nmat2875.

The role of collagen in bone apatite formation in the presence of hydroxyapatite nucleation inhibitors

Fabio Nudelman[1], **Koen Pieterse**[2], **Anne George**[3], **Paul H. H. Bomans**[1], **Heiner Friedrich**[1], **Laura J. Brylka**[1], **Peter A. J. Hilbers**[2], **Gijsbertus de With**[1], and **Nico A. J. M. Sommerdijk**[1,*]

[1]Laboratory of Materials and Interface Chemistry and Soft Matter CryoTEM Unit, Eindhoven University of Technology, PO Box 513, 5600 MB Eindhoven, The Netherlands [2]Biomodeling and Bioinformatics, Department of Biomedical Engineering, Eindhoven University of Technology, PO Box 513, 5600 MB Eindhoven, The Netherlands [3]Department of Oral Biology, University of Illinois, Chicago, USA

Abstract

Bone is a composite material, in which collagen fibrils form a scaffold for a highly organized arrangement of uniaxially oriented apatite crystals[1,2]. In the periodic 67 nm cross-striated pattern of the collagen fibril[3–5], the less dense 40-nm-long gap zone has been implicated as the place where apatite crystals nucleate from an amorphous phase, and subsequently grow[6–9]. This process is believed to be directed by highly acidic non-collagenous proteins[6,7,9–11]; however, the role of the collagen matrix[12–14] during bone apatite mineralization remains unknown. Here, combining nanometre-scale resolution cryogenic transmission electron microscopy and cryogenic electron tomography[15] with molecular modelling, we show that collagen functions in synergy with inhibitors of hydroxyapatite nucleation to actively control mineralization. The positive net charge close to the C-terminal end of the collagen molecules promotes the infiltration of the fibrils with amorphous calcium phosphate (ACP). Furthermore, the clusters of charged amino acids, both in gap and overlap regions, form nucleation sites controlling the conversion of ACP into a parallel array of oriented apatite crystals. We developed a model describing the mechanisms through which the structure, supramolecular assembly and charge distribution of collagen can control mineralization in the presence of inhibitors of hydroxyapatite nucleation.

The role of the collagen matrix[12–14] during the infiltration of the fibrils with amorphous calcium phosphate (ACP) and its subsequent transformation into oriented crystals of apatite is still unknown. Although crystal nucleation is believed to be directed by non-collagenous proteins[6,7,9–11] (NCPs), collagen has also been proposed to nucleate apatite[13,14]. So far, however, this hypothesis could not be experimentally substantiated, and collagen is generally considered a passive scaffold and template for mineral formation[16,17]. Providing

*Correspondence and requests for materials should be addressed to N.A.J.M.S. N.Sommerdijk@tue.nl.

Author contributions

F.N. carried out most experiments and co-wrote the manuscript. K.P. and P.A.J.H. carried out the molecular modelling. A.G. provided the C-DMP1 and the expertise in the work with the protein. L.J.B. contributed to the development of the mineralization experiments for cryoTEM. P.H.H.B. provided support with the cryoTEM. H.F. provided support with the tomographic reconstructions. G.W. and N.A.J.M.S. supervised the project and N.A.J.M.S. co-wrote the manuscript. All authors discussed the results and revised the manuscript.

Additional information

The authors declare no competing financial interests. Supplementary information accompanies this paper on www.nature.com/naturematerials. Reprints and permissions information is available online at http://npg.nature.com/reprintsandpermissions.

experimental evidence for the role of collagen in guiding mineral formation requires monitoring the mineralization of the collagen matrix at the molecular level. Investigating details of collagen mineralization using *in vivo* models has been proved very challenging owing to the complexity of the biological systems[6,7,9]. Recently, *in vitro* collagen mineralization was achieved by substituting the NCPs with either polyaspartic acid (pAsp) or fetuin, both inhibitors of hydroxyapatite crystallization[18–20]. These additives were shown to be instrumental in the intrafibrillar formation of oriented apatite crystals, exhibiting X-ray and electron diffraction patterns similar to those of bone apatite. Combining these *in vitro* systems with cryogenic transmission electron microscopy (cryoTEM), cryogenic electron tomography and low-dose selected-area electron diffraction (LDSAED) we studied collagen mineralization with nanometre-scale resolution, applying plunge-freeze vitrification to ensure the close-to-native preservation of the molecular structures[15].

Type I collagen from horse tendon was reconstituted into isolated fibrils on TEM grids and incubated in buffered mineralization solutions containing $CaCl_2$, K_2HPO_4 and pAsp, as described previously[19] (Supplementary S1 and S2, Fig. S1). After 72 h, cryogenic electron tomography of mineralized collagen showed the presence of plate-shaped crystals (2–5 nm thick, 15–55 nm long and 5–25 nm wide) inside the collagen fibril (Fig. 1 and Supplementary S3 and S4, Fig. S2), consistent with what is found in bone[19]. Control experiments without additives resulted in apatite crystals randomly formed in solution and on the surface of the fibrils (Supplementary S5, Fig. S3).

To investigate how the apatite crystals form inside the fibril, we carried out a time-resolved study starting from the earliest stages of mineral formation. After 24 h of mineralization calcium phosphate particles were found outside the fibril, associated with the overlap region, in close proximity to the gap zone (Fig. 2a). Cryogenic energy-dispersive X-ray spectroscopy confirmed that these precipitates are indeed composed of calcium phosphate, and LDSAED showed a diffuse band characteristic of ACP (Supplementary S6, Fig. S4). After 48 h, apatite crystals started to develop within a bed of ACP (Fig. 2b, Supplementary S6, Fig. S5) and after 72 h, elongated electron-dense crystals were abundant within the fibril, in many cases still embedded within a less dense matrix (Fig. 2c). LDSAED demonstrated that the mineral phase consisted of both ACP and oriented apatite, the latter identical to bone apatite[19] (Supplementary S6, Fig. S5). As observed previously[21], the collagen fibrils expanded in the direction perpendicular to its long axis, becoming deformed by the developing mineral (Supplementary S7, Fig. S6).

To understand the role of collagen in controlling mineral formation at the molecular level, we correlated our observations with the ultrastructure of the collagen fibril. For this we combined cryoTEM with uranyl acetate staining[22], where uranyl acetate binds to both the negatively and positively charged amino acids in the fibrils, thus significantly increasing the local mass density, and hence the image contrast[23,24]. The resulting staining pattern was consistent with previous studies using conventional TEM; that is, the banding pattern along the 67 nm repeat matched with the positions of the charged amino acids in the crystal structure of collagen[5,24] (Fig. 3a,b, Supplementary S8, Fig. S7). Furthermore, the staining did not affect the mineral phase, because the same degree of mineralization was observed as for unstained samples (Fig. 2).

After 24 h of mineralization, ACP was observed surrounding and entering the fibril, associated to the a-bands (Fig. 1b, black circle and Fig. 3b–e). These bands are ~9 nm wide and span both the overlap and gap zones at the C-terminal region of the collagen molecules[14]. Analysis of the intensity profile shows the increase and the broadening of the peaks corresponding to the a-bands, such that the a1 to a3 bands fused and became almost indistinguishable (Fig. 3e).

The infiltration of mineral into the fibril through the a-band region is not dependent on the availability of space. Gaps within the microfibril are present throughout the whole 67 nm repeat, both in the gap and overlap regions[13] (Fig. 4a), and could provide entry sites for the mineral phase into the fibril. Therefore, the site-specific localization of mineral infiltration must result from a specific interaction between the amorphous mineral phase and the collagen at this location. Indeed, whereas ACP-polyasp forms a negatively charged complex (Fig. 4c), the gaps within the a-band region that serve as entry sites for the ACP into the fibril are located within a 6 nm domain of high positive net charge (Supplementary S8, Fig. S8). This site possesses the lowest electrostatic potential energy in the microfibril for interaction with the negatively charged complex (Fig. 4b) and is therefore the most favourable region for an attractive interaction with the negatively charged complex. This suggests that the attraction between these positively charged sites and the negatively charged calcium phosphate–pAsp complex plays a critical role in mediating the entry of the ACP into the collagen.

Uranyl acetate staining was also used to identify the crystal nucleation sites within the collagen fibril. Apatite nanocrystals in their early stages were always observed on a staining band (Fig. 3c). Analysis of cryoTEM images showed that these nanocrystals were distributed evenly between the gap and overlap regions, with a small preference for the d-band in the gap zone (Fig. 3f). These results show that once ACP enters the fibril, the collagen is controlling nucleation either directly, with the charged amino acids acting as nucleation sites for apatite formation, or indirectly. As it has been shown that pAsp infiltrates the fibril[25], it is possible that the bands of charged amino acids provide locations to which the polymer–ACP complex binds and subsequently induce nucleation.

To investigate this, collagen was mineralized in the presence of fetuin. This protein induces collagen mineralization by inhibiting calcium phosphate precipitation in solution and thus allowing the mineral phase to penetrate into the fibril (Supplementary S9, Fig. S9; refs 20,26). The protein itself cannot diffuse into the fibril owing to its large molecular weight (48 kDa; ref. 27); however, zeta-potential measurements show that it forms a negatively charged complex with calcium phosphate, with a net charge of -14.5 ± 11.2 mV. In the presence of fetuin, oriented apatite crystals were formed inside the fibril with morphologies and orientation similar to the ones observed in the presence of pAsp (Supplementary S9, Fig. S10) and the nucleation of the intrafibrillar crystals again occurred exclusively on the staining bands, although no ACP formation could be detected. Our observations now show that collagen indeed induces the oriented nucleation of apatite, without the involvement of NCPs or other control agents, as previously proposed[13,14]. This further experimentally confirms computer simulations that showed how specific regions in collagen induce the formation of oriented ion aggregates with motifs corresponding to the apatite structure[28]. Our results therefore support the notion that the spatial arrangement of the charged groups in the collagen fibril provides a structural template that induces oriented apatite nucleation[14], with the *c* axis of the crystals aligned parallel to the long axis of the fibril (for a more detailed discussion see Supplementary S10). This also implies that in the present system, the main function of pAsp and fetuin is to form a stable complex with calcium phosphate, allowing it to enter the collagen fibril.

It seems, however, unlikely that in biology the function of the complex mixture of NCPs would be limited to just inhibiting extrafibrillar mineralization. This point was further investigated by carrying out the mineralization in the presence of the C-terminal fragment of the dentin matrix protein 1 (C-DMP1) which has been demonstrated to promote apatite nucleation in the presence of collagen[29] (Supplementary S11, Fig. S11). In the absence of pAsp this protein fragment induced formation of crystals only in solution and on the surface of the fibrils (Supplementary S11, Figs. S12a,b). When combined with pAsp, mineralization

occurred exclusively inside the fibrils, with apatite crystals forming from an ACP precursor phase, similar to what was observed for pAsp alone (Supplementary S11, Figs. S12c–f). However, the addition of C-DMP1 significantly accelerated mineralization, such that after 24 h the fibril already contained large amounts of apatite crystals, which again nucleated exclusively on the staining bands, equally in the gap and overlap regions (Supplementary S11, Figs S12 and S13). The absence of site-specific nucleation is surprising, as C-DMP1 also contains a site that specifically binds to the N-terminal end of collagen[29]. Hence, even in the presence of C-DMP1 crystal nucleation is controlled by collagen itself. We tentatively attribute this to the reported formation of large assemblies of this 17 kDa protein fragment in the presence of Ca^{2+} ions[30], which would be too large to penetrate the collagen fibril. How the nucleation of apatite is promoted by C-DMP1 in the present system remains unexplained for the moment.

As the formation of ACP has been proposed to proceed through the assembly of nanometre-sized clusters[31], and polymer-induced liquid-precursor phases have been described as during the precipitation of calcium phosphate in the presence of pAsp (ref. 19), we investigated the effect of this polymer on mineral formation in more detail. In control experiments without the addition of pAsp, dynamic light scattering measurements showed the rapid formation and growth of calcium phosphate particles, reaching hydrodynamic diameters (D_h) of 1,000 nm after 30 min and 5,000 nm after 2 h (Supplementary S12, Fig. S15a). At this time point, sedimentation occurred quickly, as evidenced by the decrease in count rate. CryoTEM images of samples collected after 10 min of reaction showed the presence of calcium phosphate aggregates 500 nm in size that consisted of densely packed clusters (Fig. 5a,b) of about 1 nm in size. Samples at longer reaction times could not be observed because the particles were too large and not suitable for cryoTEM analysis. In contrast, when pAsp was present in the solution, stable complexes with a D_h of 30–70 nm were formed (Supplementary S12, Fig. S15b). CryoTEM analysis revealed the presence of loosely packed assemblies of calcium phosphate clusters also of approximately 1 nm after 10 min of reaction (Fig. 5c). After 6 h, larger and denser structures were present (Fig. 5d), similar to the ones formed after 10 min without pAsp (Fig. 5b). These results show that at the early stages of mineralization, pAsp binds to and stabilizes the pre-nucleation clusters, forming loosely packed, diffuse structures that slowly aggregate and densify. The aggregates present after 6 h are similar to the ones we observed infiltrating the collagen fibril after 24 h (Fig. 2a), suggesting that these are the structures that enter the fibril.

The net negative surface charge of the pAsp–ACP complex together with the presence of positively charged regions in the collagen fibril may be essential for the mineral infiltration (Fig. 4b). Hence, *in vivo*, negatively charged NCPs may not only stabilize the amorphous phase, but may also be needed to form similar negatively charged mineral complexes, that allow the mineral to enter the collagen (for a more detailed discussion see Supplementary S13). Moreover, our studies, carried out using soft-tissue collagen, imply that the ability to mediate mineralization is not related to bone collagen but is intrinsic to type I collagen fibrils. Our results will have implications for the understanding of the process of bone biomineralization, in particular the interplay between collagen, the NCPs and the developing mineral.

Supplementary Material

Refer to Web version on PubMed Central for supplementary material.

Acknowledgments

We thank G. Falini (University of Bologna, Italy) for kindly providing the horse tendon collagen; L. B. Gower (University of Florida, Florida, USA) for a critical review of the manuscript; S. Weiner (Weizmann Institute of Science, Israel) and J. P. R. O. Orgel (Illinois Institute of Technology, Illinois, US) for helpful discussions; and J. J. van Roosmalen (Eindhoven University of Technology, The Netherlands) for his help with the tomography reconstructions. Supported by the Dutch Science Foundation, NWO, The Netherlands and by the European Community (FP6, project code NMP4-CT-2006-033277 TEM-PLANT).

References

1. Hulmes DJS, Wess TJ, Prockop DJ, Fratzl P. Radial packing, order, and disorder in collagen fibrils. Biophys. J. 1995; 68:1661–1670. [PubMed: 7612808]
2. Traub W, Arad T, Weiner S. 3-dimensional ordered distribution of crystals in turkey tendon collagen-fibers. Proc. Natl Acad. Sci. USA. 1989; 86:9822–9826. [PubMed: 2602376]
3. Hodge, AJ.; Petruska, JA. Aspects of Protein Structure. Ramachandran, GN., editor. Academic; 1963. p. 289-300.
4. Miller A. Collagen: The organic matrix of bone. Phil. Trans. R. Soc. B. 1984; 304:455–477. [PubMed: 6142488]
5. Orgel JPRO, Irving TC, Miller A, Wess TJ. Microfibrillar structure of type I collagen *in situ*. Proc. Natl Acad. Sci. USA. 2006; 103:9001–9005. [PubMed: 16751282]
6. Glimcher MJ, Muir H. Recent studies of the mineral phase in bone and its possible linkage to the organic matrix by protein-bound phosphate bonds. Phil. Trans. R. Soc. B. 1984; 304:479–508. [PubMed: 6142489]
7. Landis WJ, Song MJ, Leith A, Mcewen L, Mcewen BF. Mineral and organic matrix interaction in normally calcifying tendon visualized in 3 dimensions by high-voltage electron-microscopic tomography and graphic image-reconstruction. J. Struct. Biol. 1993; 110:39–54. [PubMed: 8494671]
8. Mahamid J, et al. Mapping amorphous calcium phosphate transformation into crystalline mineral from the cell to bone in zebrafish fin rays. Proc. Natl Acad. Sci. USA. 2010; 107:6316–6321. [PubMed: 20308589]
9. Traub W, Arad T, Weiner S. Origin of mineral crystal-growth in collagen fibrils. Matrix. 1992; 12:251–255. [PubMed: 1435508]
10. George A, Veis A. Phosphorylated proteins and control over apatite nucleation, crystal growth, and inhibition. Chem. Rev. 2008; 108:4670–4693. [PubMed: 18831570]
11. Maitland ME, Arsenault AL. A correlation between the distribution of biological apatite and amino-acid-sequence of type-I collagen. Calcif. Tissue Int. 1991; 48:341–352. [PubMed: 2054719]
12. Berthet-Colominas C, Miller A, White SW. Structural study of the calcifying collagen in turkey leg tendons. J. Mol. Biol. 1979; 134:431–445. [PubMed: 537071]
13. Katz EP, Li S. Structure and function of bone collagen fibrils. J. Mol. Biol. 1973; 80:1–15. [PubMed: 4758070]
14. Landis WJ, Silver FH. Mineral deposition in the extracellular matrices of vertebrate tissues: Identification of possible apatite nucleation sites on type I collagen. Cells Tissues Organs. 2009; 189:20–24. [PubMed: 18703872]
15. Pouget EM, et al. The initial stages of template-controlled $CaCO_3$ formation revealed by cryo-TEM. Science. 2009; 323:1455–1458. [PubMed: 19286549]
16. Stetlerstevenson WG, Veis A. Type-I collagen shows a specific binding-affinity for bovine dentin phosphophoryn. Calcif. Tissue Int. 1986; 38:135–141. [PubMed: 3011229]
17. Stetlerstevenson WG, Veis A. Bovine dentin phosphophoryn—calcium-ion binding-properties of a high-molecular-weight preparation. Calcif. Tissue Int. 1987; 40:97–102. [PubMed: 3105840]
18. Deshpande AS, Beniash E. Bioinspired synthesis of mineralized collagen fibrils. Cryst. Growth Des. 2008; 8:3084–3090.
19. Olszta MJ, et al. Bone structure and formation: A new perspective. Mater. Sci. Eng. R. 2007; 58:77–116.

20. Price PA, Toroian D, Lim JE. Mineralization by inhibitor exclusion: The calcification of collagen with fetuin. J. Biol. Chem. 2009; 284:17092–17101. [PubMed: 19414589]
21. Fratzl P, Fratzl-Zelman N, Klaushofer K. Collagen packing and mineralization—an X-ray-scattering investigation of turkey leg tendon. Biophys. J. 1993; 64:260–266. [PubMed: 8431546]
22. Beniash E, Traub W, Veis A, Weiner S. A transmission electron microscope study using vitrified ice sections of predentin: Structural changes in the dentin collagenous matrix prior to mineralization. J. Struct. Biol. 2000; 132:212–225. [PubMed: 11243890]
23. Hodge AJ, Schmitt FO. The charge profile of the tropocollagen macromolecule and the packing arrangement in native-type collagen fibrils. Proc. Natl Acad. Sci. USA. 1960; 46:186–197. [PubMed: 16590606]
24. Chapman JA, Tzaphlidou M, Meek KM, Kadler KE. The collagen fibril—a model system for studying the staining and fixation of a protein. Electron Microsc. Rev. 1990; 3:143–182. [PubMed: 1715773]
25. Jee SS, Culver L, Li YP, Douglas EP, Gower LB. Biomimetic mineralization of collagen via an enzyme-aided PILP process. J. Cryst. Growth. 2010; 312:1249–1256.
26. Rochette CN, et al. A shielding topology stabilizes the early stage protein-mineral complexes of fetuin-a and calcium phosphate: A time-resolved small-angle X-ray study. Chembiochem. 2009; 10:735–740. [PubMed: 19222044]
27. Toroian D, Lim JE, Price PA. The size exclusion characteristics of type I collagen—implications for the role of noncollagenous bone constituents in mineralization. J. Biol. Chem. 2007; 282:22437–22447. [PubMed: 17562713]
28. Kawska A, Hochrein O, Brickmann A, Kniep R, Zahn D. The nucleation mechanism of fluorapatite-collagen composites: Ion association and motif control by collagen proteins. Angew. Chem. Int. Ed. 2008; 47:4982–4985.
29. He G, George A. Dentin matrix protein 1 immobilized on type I collagen fibrils facilitates apatite deposition *in vitro*. J. Biol. Chem. 2004; 279:11649–11656. [PubMed: 14699165]
30. He G, et al. Spatially and temporally controlled biomineralization is facilitated by interaction between self-assembled dentin matrix protein 1 and calcium phosphate nuclei in solution. Biochemistry. 2005; 44:16140–16148. [PubMed: 16331974]
31. Posner AS, Betts F. Synthetic amorphous calcium phosphate and its relation to bone mineral structure. Acc. Chem. Res. 1975; 8:273–281.

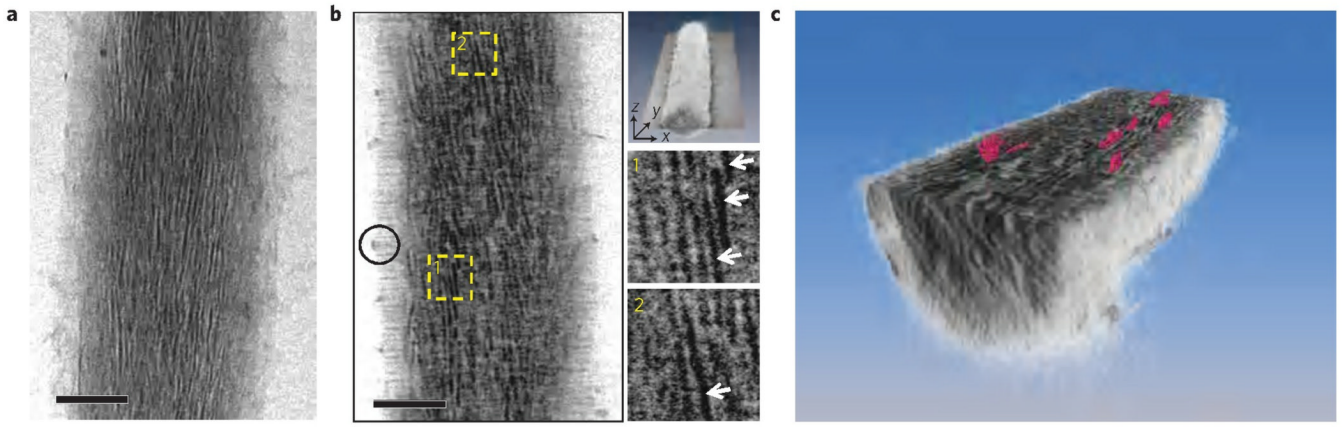

Figure 1. Cryo-electron tomography of a collagen fibril mineralized in the presence of 10 μg ml^{-1} of pAsp for 72 h and stained with uranyl acetate

a, Two-dimensional cryoTEM image. **b**, Slice from a section of the three-dimensional volume along the *xy* plane (top-most inset), where crystals are visible edge-on (insets 1 and 2, white arrows). Black circle: ACP infiltrating the fibril (see below). **c**, Computer-generated three-dimensional visualization of mineralized collagen. The fibril is sectioned through the *xy* plane, revealing plate-shaped apatite crystals (coloured in pink) embedded in the collagen matrix. Scale bars: 100 nm.

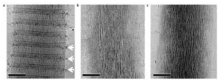

Figure 2. CryoTEM images of collagen at different stages of mineralization in the presence of 10 μg ml^{-1} of pAsp

a, Mineralization for 24 h. **b**, Mineralization for 48 h. **c**, Mineralization for 72 h. Scale bars: 100 nm.

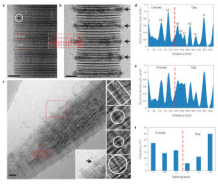

Figure 3. Uranyl acetate map of the different stages of collagen mineralization in the presence of 10 μg ml^{-1} of pAsp

a, CryoTEM image of stained, non-mineralized collagen. Staining bands are labelled according to ref. 24. White circle: 10 nm gold marker for electron tomography. **b**, CryoTEM image of stained collagen, mineralized for 24 h. Calcium phosphate is associated to the fibril in a regular pattern, following the staining bands (black arrows). Peaks are labelled corresponding to their respective staining band. **c**, CryoTEM image of a stained fibril mineralized for 48 h. Apatite crystals are found within an amorphous calcium phosphate bed, which can still be seen infiltrating into the fibril through the a-band (inset 1, black arrow). Insets 2–5 show crystals nucleating on the staining bands. **d**, Intensity profile of **a**, non-mineralized collagen. **e**, Intensity profile of **b**, collagen mineralized for 24 h. **f**, Histogram of the distribution of the number of nucleating crystals per staining band. Scale bars: 50 nm.

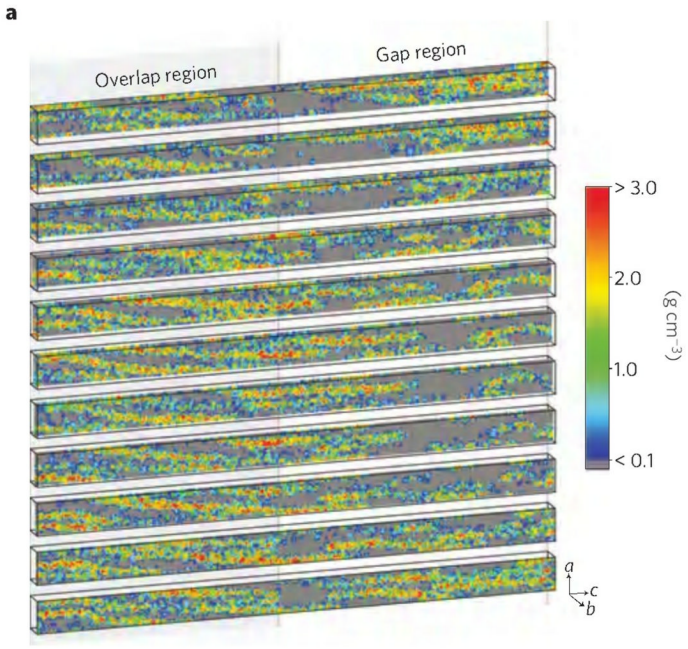

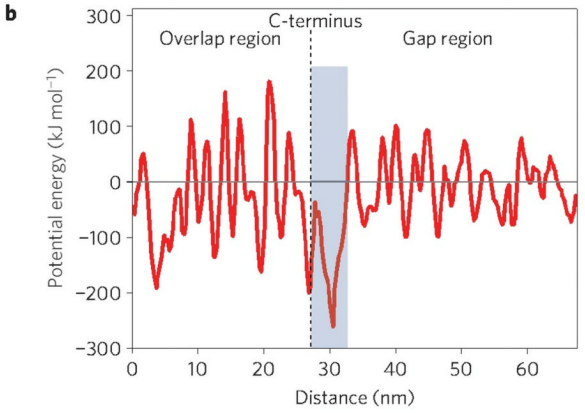

c

	Net charge (mV ± zeta-deviation)	Count rate (kpcs)
HEPES buffer	−11 ± 14	48
Polyaspartic acid	−11 ± 5	112
Calcium phosphate	4 ± 3	24,341
Calcium phosphate + polyaspartic acid	−20 ± 3	12,205

Figure 4. Analysis of the mass density and electrostatic potential energy of a microfibril, based on the crystal structure[5]

a, Mass density map of a microfibril, depicting slices through the *b* axis of the crystal unit cell. Grey areas demonstrate the space within the microfibril through which the mineral phase could potentially diffuse. **b**, Electrostatic potential energy of the empty voxels along the microfibril. The blue-shaded area indicates the region where the potential energy is lowest, meaning that it is the most favourable for interaction with negative charges. This region is close to the C-terminus (dashed line) and corresponds to the mineral infiltration site, that is, the a-bands **c**, Zeta-potential measurements of the mineral phase and the other solution components, illustrating the negative charge of the pAsp–mineral complex. The high zeta-deviation and low count rate of pure HEPES buffer and pure pAsp show that they are not contributing to the measurements of the calcium phosphate and calcium phosphate–pAsp complexes.

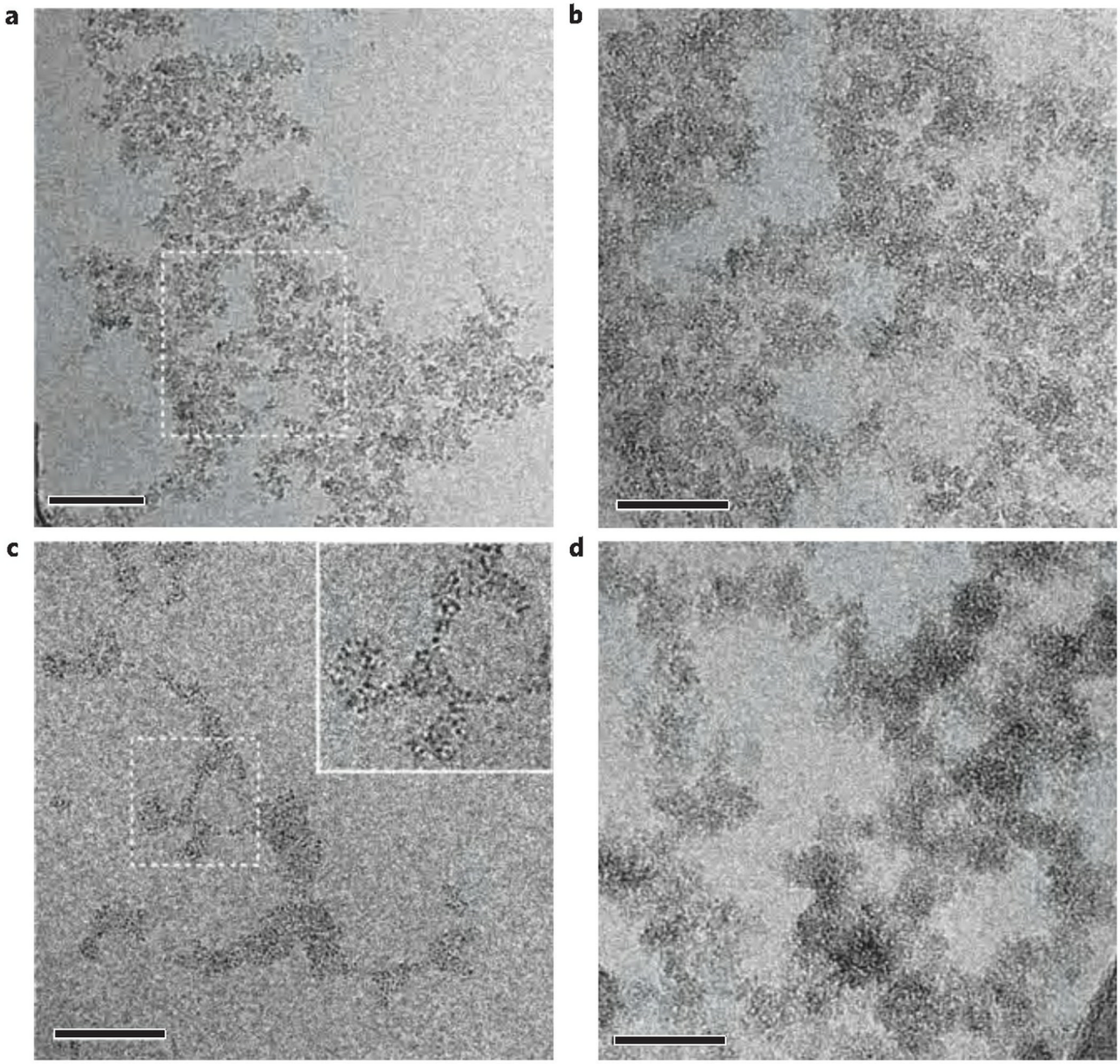

Figure 5. Analysis of calcium phosphate precipitation in the absence and presence of pAsp

a, CryoTEM image of calcium phosphate aggregates formed after 10 min of reaction without pAsp. Scale bar: 100 nm. **b**, Higher magnification of the area marked in **a**. Scale bar: 50 nm. **c**, CryoTEM image of calcium phosphate aggregates formed after 10 min of reaction in the presence of pAsp. Scale bar: 50 nm. **d**, CryoTEM image of calcium phosphate aggregates formed after 6 h of reaction in the presence of pAsp. Scale bar: 50 nm.